JOURNAL OF VIROLOGY, Sept. 2007, p. 9922–9931 Vol. 81, No. 18
0022-538X/07/$08.00+0 doi:10.1128/JVI.00988-07

Human Papillomavirus Type 31 Uses a Caveolin 1- and Dynamin 2-Mediated Entry Pathway for Infection of Human Keratinocytes[▽]

Jessica L. Smith, Samuel K. Campos, and Michelle A. Ozbun*

Department of Molecular Genetics and Microbiology, The University of New Mexico School of Medicine, Albuquerque, New Mexico 87131

Received 7 May 2007/Accepted 29 June 2007

Papillomaviruses are species-specific and epitheliotropic DNA viruses that cause tumors in their natural hosts. Certain infections with genital human papillomavirus (HPV) types are causally related to cervical cancer development. Most papillomaviruses are thought to infect cells via a clathrin-dependent pathway, yet no studies have determined the entry route in permissive host epithelial cells. Employing fluorescently labeled and native virions, we tested the effects of dominant-negative and biochemical inhibitors of cellular endocytosis pathways. Infections of human keratinocytes, a natural host cell type for HPVs, were assessed visually and by infectious entry assays. We found that HPV type 31 (HPV31) entry and initiation of early infection events require both caveolin 1 and dynamin 2 and occur independently of clathrin-mediated endocytosis. Treatment with chlorpromazine and filipin had opposing effects on HPV31 and HPV16 infection. HPV31 entry was remarkably slow, with a half-time of ≈14 h, whereas the entry half-time of HPV16 was 4 h. Consistent with a caveola-mediated entry pathway for HPV31, the virions associated with detergent-resistant lipid rafts. During a 16-h microscopic tracking of HPV31 and HPV16 virions, no colocalization of the two viral types was observed. These data suggest that HPV31 and HPV16 virions use distinct routes for host epithelial cell entry.

Human papillomaviruses (HPVs) are small nonenveloped viruses that encapsidate a double-stranded circular DNA genome of ≈8 kb. HPVs display strict species and cell type specificity, infecting human keratinocytes (HKs) exclusively in nature. The association between high-risk HPVs (i.e., HPV16, -18, -31, and -45) and cervical cancer is well established, as >99% of cervical cancers are positive for HPV DNA (3). Additionally, these HPV types have been linked to ≥20% of head and neck cancers (15, 21).

A number of qualities that permit HPV persistence in vivo have impeded research, leaving many basic aspects of HPV biology poorly understood. HPVs have an absolute requirement for differentiating epithelia for life cycle completion and thus cannot be grown or studied to a great extent in traditional cell culture. Low-level replication and protein expression during early infection hinder detection of HPV infection. This has prompted many researchers to study the interaction of HPV pseudovirions (PsVs) or virus-like particles (VLPs) with nonrelevant cell types. However, this has resulted in confusion as to the natural infectious pathway used by high-risk HPVs. For example, Giroglou et al. found that interaction of HPV type 16 and 33 PsVs with heparan sulfate proteoglycans (HSPGs) was required for infection as measured by reporter gene expression in COS-7 cells, a monkey kidney cell line (22). To determine whether HSPG mediates HPV infection in host HKs, we used authentic HPV31 virions produced in the organotypic system. Infection was measured by quantification of a spliced predominant early viral RNA, E1^E4 (35, 36). Using the same experimental design as Giroglou et al., we confirmed that HPV31 infection of COS-7 cells required HSPG. However, we also demonstrated that HPV31 virion interactions with cell surface HSPG was not required for infection of HKs (37). These findings underscore the importance of using relevant cell types and authentic virions to study viral early infection events.

Viruses generally enter cells by way of receptor-mediated endocytosis (46). The well-characterized clathrin-dependent pathway for ligand endocytosis has long been recognized as the major route used by many nonenveloped viruses to enter cells. Entry via this pathway proceeds through endosomes, and the decreasing pH of these vesicular compartments (20) often acts to stimulate endosomal escape (46). A clathrin-independent entry pathway involves caveolae and provides an advantage of access to signaling centers at the cell surface and direct delivery to caveosomes, which can mediate transport to several cellular organelles where uncoating may occur. There are examples of highly related viruses using different infection routes. For example, the polyomaviruses simian virus 40 (SV40) and BK virus use a caveola-mediated pathway for cellular entry (1, 40), whereas their closely related counterpart JC virus initially employs a clathrin-dependent route (16).

The endocytic requirements for HPV entry have not been studied in HKs. HPV16 VLPs were found to colocalize with BPV1 VLPs and virions, and these particles enter mouse C127 cells via clathrin-dependent endocytosis with a relatively long internalization time (half-time [$t_{1/2}$] of ≈4 h) (13). In COS-7 cells, HPV16 and HPV58 PsV entry was clathrin dependent, while HPV31 entry was caveola dependent (5). However, a recent publication showed clathrin-dependent and caveola-independent entry of both HPV16 and HPV31 into COS-7 cells as well as 293TT cells, a simian virus 40 (SV40) large T-antigen-transformed human kidney cell line (27). Although some of these studies were performed in human cells, none of the cell types is relevant to natural HPV infection.

* Corresponding author. Mailing address: Department of Molecular Genetics and Microbiology, The University of New Mexico School of Medicine, Albuquerque, NM 87131. Phone: (505) 272-4950. Fax: (505) 272-9912. E-mail: mozbun@salud.unm.edu.

▽ Published ahead of print on 11 July 2007.

In the current study, our goal was to determine the internalization pathway used by infectious HPV31 virions in their host cell type, HKs. We first examined the time course of HPV31 entry into several cell lines relevant to natural HPV infection and found it to be extremely slow, even compared to HPV16 internalization. Monitoring the effects of dominant-negative inhibitors of clathrin- and caveola-dependent endocytosis on HPV31 entry and infection, we found both caveolin 1 and dynamin 2 to be important mediators. Inhibition of clathrin-mediated endocytosis did not affect HPV31 entry or initiation of viral early gene transcription. Infections with HPV31 and HPV16 in the presence of the clathrin-mediated endocytosis inhibitor chlorpromazine or caveola-mediated endocytic inhibitor filipin confirmed that HPV31 entry was caveola dependent, whereas HPV16 entered HKs through clathrin-dependent endocytosis. Consistent with caveola-mediated entry, HPV31 virions associated with detergent-resistant microdomains (DRMs). Conversely, HPV16 displayed low DRM association. We conclude that HPV31 entry into host HKs is lipid raft mediated and occurs by way of caveolae. These entry requirements differ from those reported for HPV16 (13) and our observations with HPV16 virions in HKs. These data suggest that HPV31 and HPV16 may use different pathways to enter cells. Furthermore, when observing fluorescently labeled HPV31 and HPV16 virions upon binding and entry into HKs, at no time during entry did the two HPV types colocalize. These data support the hypothesis that HPV31 and HPV16 use distinct entry pathways to infect HKs.

MATERIALS AND METHODS

Cell culture and transfections. HaCaT cells are a spontaneously immortalized epithelial line derived from normal adult skin (4). HEK-293T cells are derived from a human embryonic kidney cell line immortalized with SV40 large T antigen. Cells were maintained in Dulbecco's modified Eagle's medium–Ham's F-12 nutrient mixture containing 10% fetal calf serum, 4× amino acids, 2 mM L-glutamine, 100 U/ml penicillin, and 1 μg/ml streptocymin (Sigma). End1E6/E7 and Ect1E6/E7 cells were derived from normal endocervical and ectocervical tissues and immortalized with HPV16 E6 and E7 proteins (18). Low-passage human foreskin keratinocytes were pooled from three donors and cultured as described previously (37). Plasmids encoding wild-type and dominant-negative proteins tagged with green fluorescent protein (GFP) have been reported: caveolin 1 (39), Eps15 mutants (2), and dynamin 2 (33). HaCaT cells were transfected using the Nucleofector kit (Amaxa). Briefly, cells were tryspinized, pelleted, and resuspended in 100 μl transfection solution V with 4 μg of DNA per reaction. Following electroporation, cells were seeded onto coverslips in 6-well plates or in 12-well plates. Entry studies and infections were assessed at 48 h posttransfection.

Virion production and purification. HPV31 virions were obtained from organotypic cultures of CIN-612 9E cells as previously described (35, 36). The transfection-based method for papillomavirus production was modified from that previously published (41). 293T cells were transfected by the calcium phosphate method with recircularized HPV31 genome and codon-optimized HPV31-L1/L2-expressing plasmid. At 48 h posttransfection, cells were tryspinized, pelleted, and resuspended at 1×10^8 cells/ml in Dulbecco's phosphate-buffered saline (PBS)–9.5 mM $MgCl_2$. Cells were lysed and subjected to three freeze-thaw cycles; DNase treatment and virion maturation were handled as described previously (41). Supernatants were layered atop a 1.25-g/ml to 1.4-g/ml step CsCl gradient. Following centrifugation at 20,000 × *g* for 16 to 18 h, the viral band was extracted by side puncture. Virions were dialyzed twice at 4°C against HSB (25 mM HEPES [pH 7.5], 500 mM NaCl, 0.02% Brij58, 1 mM $MgCl_2$, 100 μM EDTA, 0.5% ethanol). Virions were concentrated using an Amicon Ultra-4 100,000-molecular-weight centrifugal filter (Millipore) as needed. Virion stocks were quantified by dot blotting based upon viral genome equivalents (vge) as previously described (35, 36). Virion purity was assessed by sodium dodecyl sulfate-polyacrylamide gel electrophoresis (SDS-PAGE) and Coomassie staining and by transmission electron microscopy (TEM). Virus stocks were visualized by TEM (Hitachi 7500) at 80 kV following binding to a carbon-coated electron microscopy grid and negative staining with 2% uranyl acetate.

Infections. Cells were exposed to virion stocks as previously described (35, 36). Briefly, stocks were sonicated at 0°C and diluted in media. Viral inocula were added to HaCaT cells and incubated at 4°C for 1 h with rocking to permit viral attachment. Inocula were aspirated, cells were washed with media, and fresh media were added. Cells were incubated at 37°C for various times before harvest. In virus neutralization experiments, H31.A6 monoclonal immunoglobulin G1 (IgG1) antibody to HPV31 VLPs (7) was diluted 1:1,000 in medium and added to cells at the times indicated postattachment. Infections in the presence of endocytic inhibitors were performed after pretreatment with each inhibitor for 1 h at 37°C. Inhibitors were present in media during viral attachment and throughout 48 h of incubation at 37°C following attachment. The chlorpromazine (Calbiochem) concentrations used were 10 and 20 μM. The filipin III (Sigma) concentrations used were 0.8 and 1.6 μM.

RNA isolation and RT-qPCR analysis. Total RNAs were extracted from cells using TRIzol (Invitrogen), and nucleic acid concentrations were determined by spectrophotometer. Reverse transcription (RT) of total RNAs (2 to 3 μg) and triplicate quantitative PCR (qPCR) reactions were performed using GeneAmp RNA PCR reagents and AmpliTaq Gold DNA polymerase (Applied Biosystems) using qPCR primers, probes, and conditions as previously described (35–37). Acceptable slope values were between −3.2 and −3.5, and correlation values were between −0.9800 and −0.9999. Results are shown as the average of three values falling between 0 and 4 standard deviations of the threshold cycle value. Error bars represent the standard error of the mean (SEM).

Virion labeling with fluorescent dyes. Approximately 1 μg of Alexa Fluor 594 (AF594) or AF488 carboxylic acid succinimidyl ester (Molecular Probes) was mixed with 10^8 virions (vge) and incubated for 1 h at room temperature. Labeled stocks were washed three times with 1× HSB and recovered using a Millipore Amicon Ultra-4 centrifugation filter to remove unincorporated dye.

Fluorescent virion entry studies. Cells were seeded at 5,000 cells/slip onto coverslips in six-well plates 1 day prior to binding. AF594-HPV31 virions were diluted in medium, added to prechilled cells, and allowed to attach for 1 h on ice at 5,000 to 10,000 vge/cell. Following binding, virus was removed, and cells were washed with medium before addition of fresh medium. For dominant-negative inhibitor studies, virus was bound to cells at 48 h posttransfection and cells were incubated at 37°C for 24 h. Fixation was with 2% paraformaldehyde–PBS for 15 min at room temperature. Coverslips were slide mounted using Vectashield plus 4′,6′-diamidino-2-phenylindole (DAPI; Vector Labs). Microscopy photos were taken on a Zeiss META confocal microscope with a ×63 objective.

DRM association assay and flotation gradient centrifugation. AF594-labeled transferrin (TF [Molecular Probes]), AF594-cholera toxin B (CT-B [Molecular Probes]), AF594-HPV31, or AF594-HPV16 was bound to cells seeded onto coverslips for 1 h at 4°C, before incubation at 37°C for indicated times in the presence or absence of 10 mM methyl-β cyclodextrin (MβCD [Sigma]) as previously described (12, 42). Cells were then incubated with PBS or 1% Triton X-100 (TX-100) on ice for 10 min before paraformaldehyde fixation. Coverslips were slide mounted with Vectashield plus DAPI (Vector Labs) and viewed on a Zeiss META confocal microscope. Alternatively, unlabeled virions were cell bound in the presence or absence of 10 mM MβCD (Sigma) as described above, and flotation gradient centrifugation was performed as previously described (42). Cells were harvested in lysis buffer (20 mM Tris-Cl [pH 7.4], 150 mM NaCl, 1% NP-40, 0.25% sodium deoxycholate, 1 mM EDTA, 1 mM phenylmethylsulfonyl fluoride, 1× protease inhibitor, 1 mM sodium orthovanadate), sonicated, and Dounce homogenized, and cellular debris was pelleted. Supernatants were layered under a discontinuous 40/30/5% Optiprep gradient and centrifuged at 40,000 rpm in an SW41 rotor. Fractions were collected from the top and analyzed by 10% SDS-PAGE and Western blotting for HPV31 L1 with polyclonal anti-HPV31 L1 antisera.

RESULTS

HPV31 production and infectivity. For years, HPV virion production was only possible using systems that yield differentiated epithelial tissue, such as the organotypic culture system (32) or the mouse xenograft model (29). These systems are limited by technical difficulty and expense and typically result in low virion yields. Recent advances permit complete HPV virion production using a transfection-based, differentiation-independent method (41). Papillomavirus virions produced in

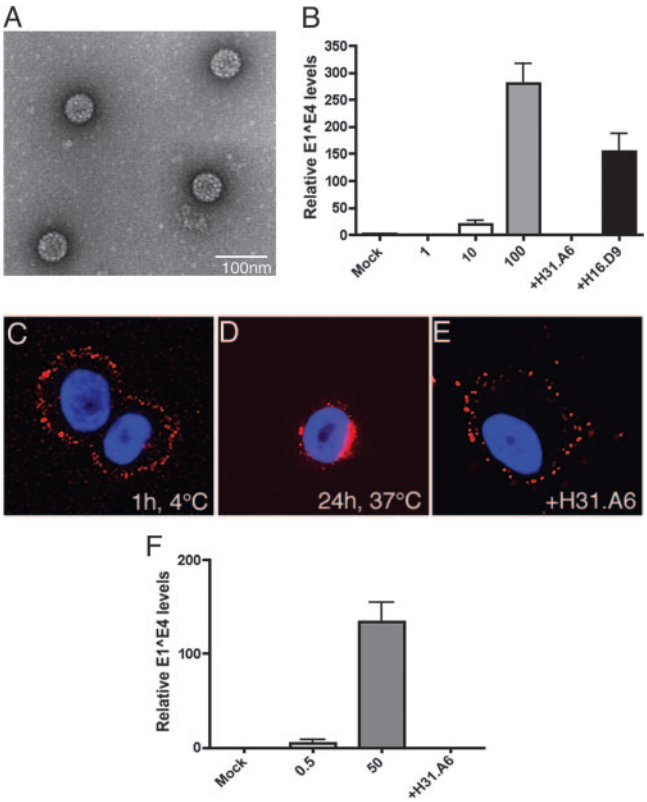

FIG. 1. HPV31 virions produced by a transfection-based method display normal morphology and infectivity properties. (A) Transfection-derived HPV31 virions visualized by TEM. (B) HaCaT cells were exposed to increasing doses of HPV31 (1, 10, and 100 vge/cell) as described in Materials and Methods. Monoclonal antibodies H31.A6 and H16.D9 were diluted in media and added to cells immediately following viral attachment. Total RNAs were subjected to RT-qPCR in triplicate to quantify spliced HPV31-E1ˆE4 transcripts indicative of infection (48 h p.i.). Error bars represent SEM. (C) AF594-labeled HPV31 (red) was bound to HKs at 10,000 vge/cell and visualized after 1 h at 4°C, after incubation at 37°C for 24 h (D), or after incubation at 37°C for 24 h in the presence of H31.A6 neutralizing antibody (E). Coverslips were mounted in the presence of DAPI to visualize nuclei. (F) HaCaT cells were inoculated with AF594-labeled HPV31 at the indicated doses; neutralizing antibody H31.A6 was used as in panels B and E. Infection was quantified as in panel B.

this system are indistinguishable from tissue-derived virions in infectivity kinetics and clinical outcome in an in vivo animal model (11). We used this method to produce infectious HPV31 virions that display normal morphology and infectivity properties (Fig. 1). Virions were quantified by dot blotting for vge and by Coomassie blue staining following SDS-PAGE with protein standards to estimate capsid equivalents. We reproducibly produced 1,000 to 5,000 capsids per vge. Similar to what we find with tissue-derived HPV31 (35–37), we detected a dose-dependent increase in HPV31-E1ˆE4 transcript levels by RT-qPCR following human keratinocyte infection with increasing HPV31 doses. Additionally, postattachment treatment with H31.A6, an HPV31 neutralizing antibody, completely blocked infection, while an HPV16-specific antibody did not significantly inhibit infection (Fig. 1B). These data further confirm that virions produced by this transfection-based method display infectivity properties indistinguishable from those produced in tissue-based systems.

AF-labeled virions as a tool to study cellular entry. Experiments were performed to determine the utility of AF594 fluorescent virion labeling and whether the label might affect early infection events (Fig. 1C to F). We first tested entry of AF594-HPV31 and the effect of adding a neutralizing antibody postattachment (Fig. 1C to E). AF594-HPV31 binding at the surface of HKs was readily visualized when cells were exposed to ≈10,000 vge per cell after 1 h at 4°C (Fig. 1C). As previously reported (8, 14), we observed that a clear majority of fluorescent virions bound to the extracellular matrix secreted by HKs and remained bound throughout incubation. The focal point at which images were taken was in the central plane of the cell, and thus the extracellular matrix binding is not visible. Therefore, despite the high dose of virions added to the HKs, the number of particles binding at the plasma membrane and entering cells appears to be a small fraction thereof. After incubation at 37°C for 24 h, the virus was observed distributed perinuclearly within cells (Fig. 1D). Postattachment treatment with the neutralizing antibody H31.A6 completely inhibited AF594-HPV31 entry (Fig. 1E), as AF594-HPV31 particles remained at the cell surface after 24 h at 37°C. AF594-HPV31 retained full infectivity, as measured by early viral gene expression, and infection was completely neutralized by antibody H31.A6, as expected (Fig. 1F). These data indicate that AF labeling of virions does not alter their biological properties.

HPV31 entry into HKs is slow. The internalization $t_{1/2}$ of BPV1 and HPV16 entry into mouse C127 cells was previously reported to be ≈4 h, which is slow compared to those of other viruses (13). Postattachment antibody-mediated neutralization experiments and confocal microscopy visualization of AF594-labeled virions were performed to determine the kinetics of HPV31 and HPV16 entry into HKs. Sensitivity to antibody neutralization at various times postattachment was determined in three different cell types relevant to natural HPV infection (Fig. 2A): a spontaneously immortalized epithelial line (HaCaT) (4), an ectocervical cell line (Ect1), and an endocervical cell line (End1) (18). Infections were performed by exposing cells to HPV31 for 1 h at 4°C to promote attachment but not internalization. Cells were then washed, refed with regular growth medium, and placed at 37°C to allow viral entry. Media were changed on replicate cultures at various times postinfection (p.i.), where cells received no antibody, an HPV31 neutralizing monoclonal antibody (H31.A6), or an isotype control antibody. At 48 h p.i., cells were harvested for total RNAs and RT-qPCR was used to detect and quantify HPV31 E1ˆE4 transcripts (Fig. 2A). No significant HPV31 infection inhibition was observed at any of the assayed time points with medium only or with the isotype control antibody (not shown). However, treatment of cells with antibody H31.A6 in all three cell types considerably inhibited HPV31 infection from 0 h up to 8 h after internalization was initiated by shifting to 37°C. Postattachment neutralization by H31.A6 at 12 h after temperature shift resulted in ≥50% inhibition of HPV31 infection, but the neutralizing antibody had no effect on infection by 16 h after internalization began. Identical results were obtained with differentiation- and transfection-derived HPV31 virions. By interpolation, the $t_{1/2}$ of HPV31 in HKs is ≈14 h, where half the virions remain susceptible to neutralization following at-

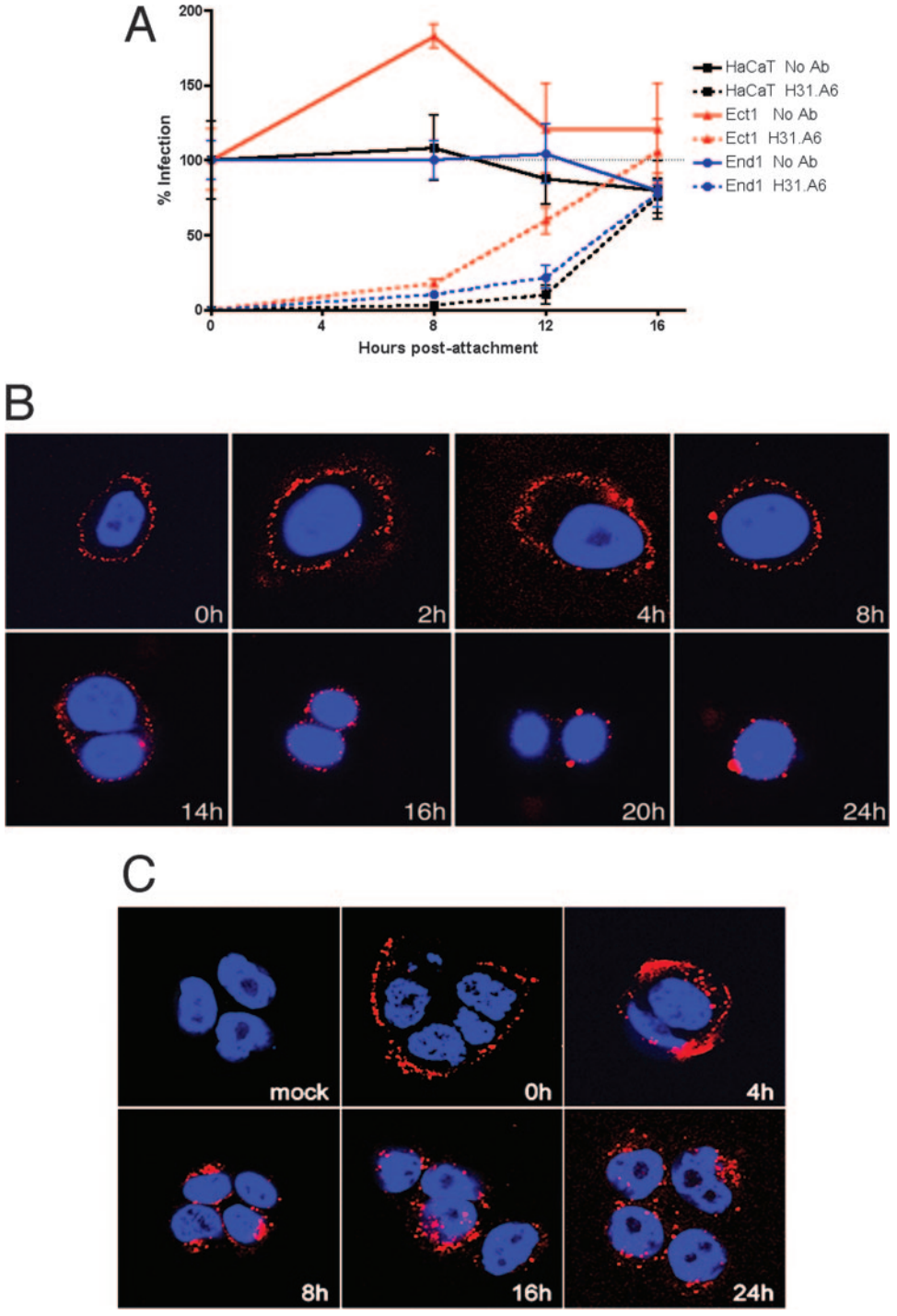

FIG. 2. Time course of HPV31 internalization. (A) Organotypic culture-derived or transfection-derived HPV31 virions were bound to HaCaT (black boxes), Ect1 (red triangles), or End1 (blue circles) cells for 1 h at 4°C at a dose of 50 vge/cell, and cells were washed and refed with regular growth media. At the indicated times postattachment, cells were treated with H31.A6 (dashed lines) or refed with new media (solid lines). The cells were harvested at 48 h p.i., and RNA was analyzed in triplicate by RT-qPCR for HPV31 E1^E4 levels; values were normalized to the average of the untreated controls at 0 h. Error bars represent SEM. Ab, antibody. (B) AF594-labeled HPV31 was bound to HaCaT cells on glass coverslips at 10,000 vge/cell for 1 h at 4°C. Cells were washed, refed with regular growth medium, and shifted to 37°C. At indicated times postattachment, cells were fixed and stained with DAPI to visualize nuclei. (C) AF594-labeled HPV16 was bound to HaCaT cells on glass coverslips at 10,000 vge/cell for 1 h at 4°C. Cells were washed, refed with regular growth medium, and shifted to 37°C. At indicated times postattachment, cells were fixed and stained with DAPI to visualize nuclei.

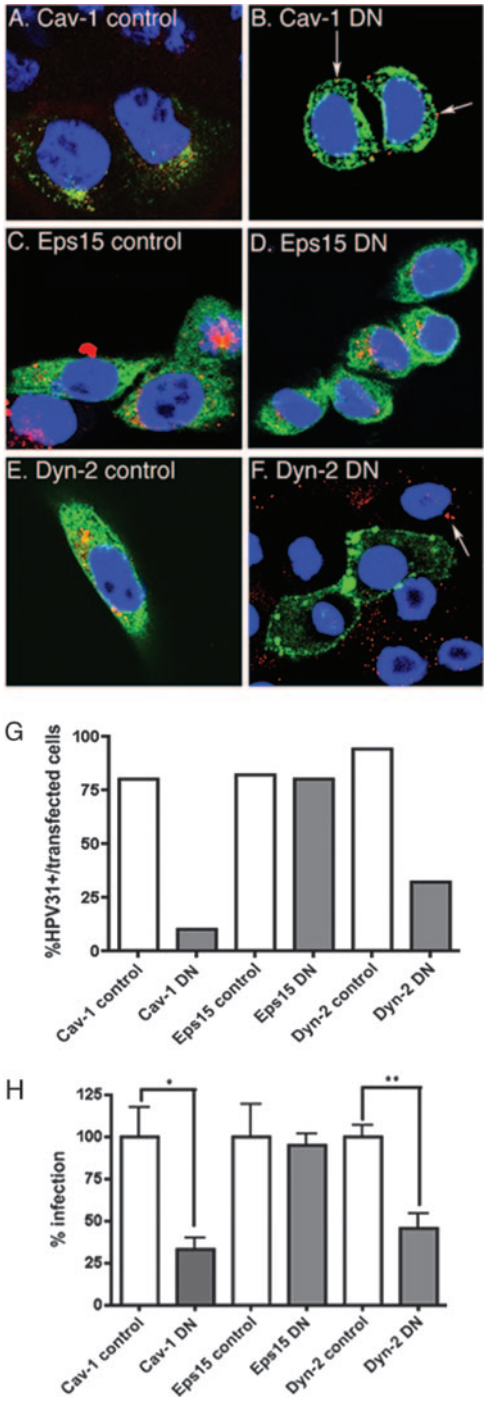

FIG. 3. Effects of dominant-negative endocytosis inhibitors on HPV31 entry and early transcription. (A to F) HaCaT cells transfected with GFP-tagged dominant-negative inhibitors of endocytosis and their corresponding controls. At 48 h posttransfection, AF594-HPV31 virions were bound to cells for 1 h at 4°C and cells were washed, refed with regular growth medium, and placed at 37°C. Cells were fixed and stained with DAPI 24 h after the 37°C shift to promote virus internalization. (A and B) Wild-type caveolin 1-GFP (Cav-1 control) and dominant-negative caveolin 1 (Cav-1 DN). (C and D) Wild-type Esp15 (Eps15 control) and Eps15 dominant-negative Eps15 (Eps15 DN). (E and F) Wild-type dynamin 2 (Dyn-2 control) and dominant negative dynamin 2 (Dyn-2 DN). Results are representative of three replicate transfection/infection experiments. (G) Quantification of HPV31 particle entry into transfected cells was performed by blinded evaluation of internalization state of AF594-HPV31 in a total of 100 transfected cells (expressing GFP). (H) Triplicate cultures of transfected HaCaT cells were infected 48 h posttransfection with HPV31 virions at 50 vge/cell. RNA isolated 48 h p.i. was quantified in triplicate for HPV31 E1^E4 transcript levels by RT-qPCR. Error bars represent SEM, and statistical significance was achieved with $P < 0.05$ (*) and $P < 0.01$ (**).

tachment, presumably as a result of retention at the cell surface signifying slow internalization.

It has been suggested that the long period of time following attachment during which some papillomaviruses are susceptible to antibody-mediated neutralization may result from neutralizing antibodies chasing the virus into vesicles and neutralizing infection postentry (10). Although some evidence supports this method of neutralization by IgA, it does not appear to be a neutralization strategy used by IgG antibodies (43). To directly observe the entry time course of viral particles, we tracked AF594-labeled virion uptake into HKs (Fig. 2B and C). Following virion attachment, the cells were washed and incubated at 37°C. At the indicated time points, cells were fixed and visualized by confocal microscopy. HPV31 was observed binding to the cell surface at 0 h postattachment and remained surface bound up to 8 h following temperature shift to induce internalization. At 14 h post-temperature shift, virions had begun to enter cells, and by 24 h postshift, all virus particles appeared to have entered the cells, where they localized perinuclearly. These data are in agreement with the results with unlabeled virions in Fig. 2A that suggest a long $t_{1/2}$ of ≈14 h for HPV31 in HKs. A more rapid internalization time for HPV16 into C127 cells has been reported (13). Our results using AF594-labeled HPV16 confirm a $t_{1/2}$ of ≈4 h for HPV16 in HKs, whereby 8-h postinternalization HPV16 particles are perinuclear (Fig. 2C). The considerable difference in internalization times displayed by the two viral types in HKs suggests that HPV31 and HPV16 may be using different cellular entry pathways in these cells.

HPV31 entry and early infection events are caveolin 1 and dynamin 2 dependent. To determine the endocytic route utilized by HPV31 to enter HKs, well-characterized dominant-negative inhibitors of various endocytic pathways were used. HaCaT cells were transfected with various wild-type- and dominant-negative-expressing constructs, and 48 h later AF594-HPV31 virions were bound and allowed to enter cells for 24 h at 37°C. Caveolin 1 tagged at the N terminus with GFP (Cav-1 DN) was previously shown to inhibit caveola-mediated endocytosis as demonstrated by blockage of SV40 entry, whereas a chimeric protein with GFP placed at the C terminus of caveolin 1 (Cav-1 control) does not display this inhibitory effect (39). In HaCaT cells, inhibition of caveola-mediated endocytosis by expression of Cav-1 DN reduced HPV31 entry and virions were visible still bound at the cell surface following 24 h at 37°C (Fig. 3B, arrows). Conversely, Cav-1 control transfected cells showed no block in HPV31 entry and AF594-HPV31 was observed at a perinuclear location (Fig. 3A). When cells were transfected with a dominant-negative inhibitor of Eps15 (Eps15 DN), a necessary adaptor for clathrin coat assembly, or its corresponding control (Eps15 control), which lacks the AP-2 binding site (2), no HPV31 entry inhibition was observed

(Fig. 3C and D). Dynamin 2, a motor protein that pinches off vesicles from the cell surface, has been observed to function in both clathrin- and caveola-mediated pathways (26, 34, 47). A well-characterized mutant of dynamin 2 (K44A) has been previously shown to inhibit dynamin 2 activity (33). Expression of GFP-dynamin-2K44A (Dyn-2 DN) appeared to have an inhibitory effect on HPV31 entry, as many transfected cells were not positive for HPV31 entry, while HPV31 entry was not inhibited in adjacent untransfected cells (Fig. 3F, arrow). Expression of wild-type dynamin 2 (Dyn-2 control) caused no blockage of HPV31 entry (Fig. 3E). HPV31 entry into transfected cells was quantified in a blinded assessment by counting the number of transfected cells positive for HPV31 entry after 24 h at 37°C (Fig. 3G). Similar results were obtained when primary human foreskin keratinocytes were transfected with each of the dominant-negative mutants or their controls (data not shown). The microscopy results indicate that clathrin-mediated endocytosis plays a negligible role in HPV31 entry, while >90% of HPV31 entry is caveolin 1 dependent. Additionally, dynamin 2 appears to mediate ~70% of HPV31 entry into HKs.

To determine whether the effects of the dominant-negative proteins on HPV31 entry observed by microscopy were a reflection of the actual infectious pathway, an infectious entry assay was performed to examine early viral transcription in transfected HaCaT cells. HKs transfected with each construct in triplicate were exposed to HPV31 virions at 50 vge/cell on day 2 posttransfection. RNA was harvested at 48 h p.i., and HPV31 E1^E4 transcripts were quantified by RT-qPCR. Although we were unable to obtain transfection efficiencies of >75%, the data from these infections confirmed the requirements for caveolin 1 and dynamin 2 that were observed in the microscopic analysis (Fig. 3H). Transfection with Cav-1 DN caused a 67% inhibition of HPV31 infection as compared to infection of Cav-1 control transfected cells, and inhibition was statistically significant. We believe that the remaining infection observed in these samples is due to incomplete transfection, although some infection may result from entry through a minor pathway that is caveola independent. Inhibition of clathrin-mediated endocytosis by transfection with Eps15 DN had no effect on HPV31 infection compared with Eps15 control transfected cells, confirming that HPV31 infection is independent of clathrin-mediated endocytosis. HPV31 infection was inhibited 55% following transfection with Dyn-2 DN as compared with Dyn-2 control transfected cells; these results were highly significant.

Biochemical inhibitors confirm clathrin-dependent HPV16 entry and caveola-dependent HPV31 entry. To verify the dependence on caveolae for HPV31 infection in HKs, as well as to confirm previous reports of clathrin-dependent HPV16 entry, infections with both viral types were performed in the presence of the well-characterized endocytic inhibitors chlorpromazine and filipin. Chlorpromazine, an inhibitor of clathrin-mediated endocytosis (48), blocked HPV16 infection in a dose-dependent manner, resulting in 72% inhibition at the highest concentration used (Fig. 4A), confirming the clathrin dependence of HPV16 infection in HKs. Treatment with chlorpromazine had a negligible effect on HPV31 infection (Fig. 4A). In contrast, treatment with filipin, a cholesterol-binding drug that blocks caveola-dependent endocytosis, inhibited HPV31 infection by 69% at the highest concentration used

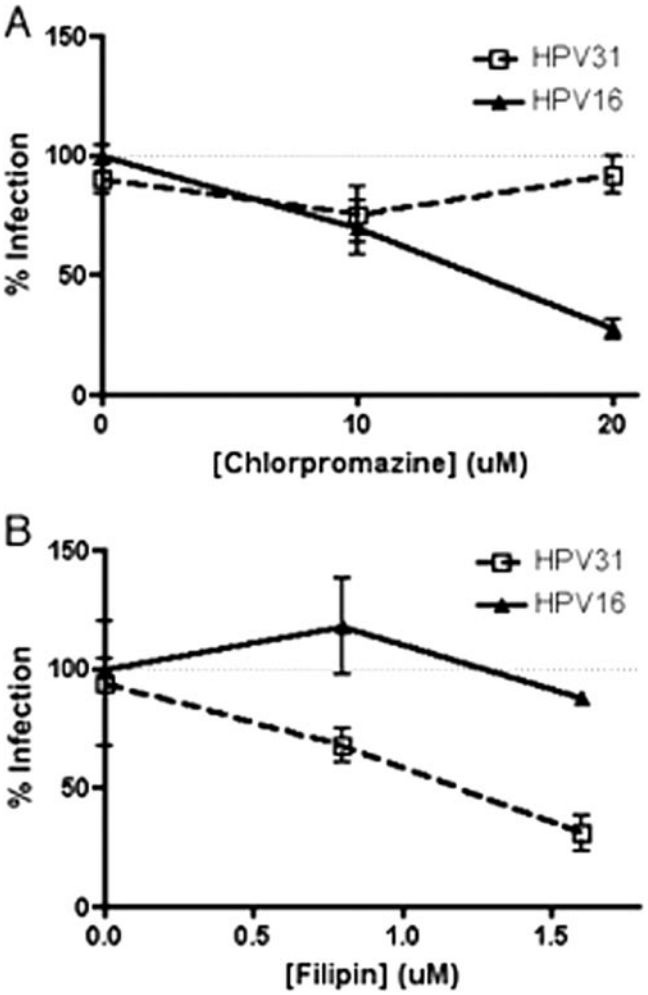

FIG. 4. Effects of biochemical endocytic inhibitors on HPV31 and HPV16 infection of HKs. HaCaT cells were pretreated with increasing concentrations of chlorpromazine (A [0, 10, and 20 μM]) or filipin (B [0, 0.8, and 1.6 μM]) for 1 h at 37°C. HPV31 (open boxes, dashed lines) or HPV16 (triangles, solid lines) virions at 50 vge/cell were bound for 1 h at 4°C to promote viral attachment. Cells were then washed, refed with medium/inhibitor, and placed at 37°C. RNA isolated at 48 h p.i. was quantified for HPV31 E1^E4 transcript levels by RT-qPCR. Infections were performed in duplicate, and RT-qPCR was performed in triplicate, with error bars representing SEM.

(Fig. 4B), while HPV16 infection was unaffected by filipin treatment (Fig. 4B). These inhibitor studies confirm that HPV31 infection of HKs is caveola dependent, while HPV16 infection is clathrin dependent.

HPV31 associates with DRMs. Lipid rafts are low-density regions of the plasma membrane where high concentrations of cholesterol localize along with glycosylphosphatidylinositol-linked proteins and several other key factors, especially caveolins. These domains typically act as signaling centers that send messages from the plasma membrane into the cell, and caveola-mediated endocytosis is thought to originate in these centers (reviewed in reference 30). One characteristic of lipid rafts is their resistance to detergent solublization; thus, they are denoted as DRMs. To investigate whether HPV31 associates with DRMs as part of caveola-mediated entry, we per-

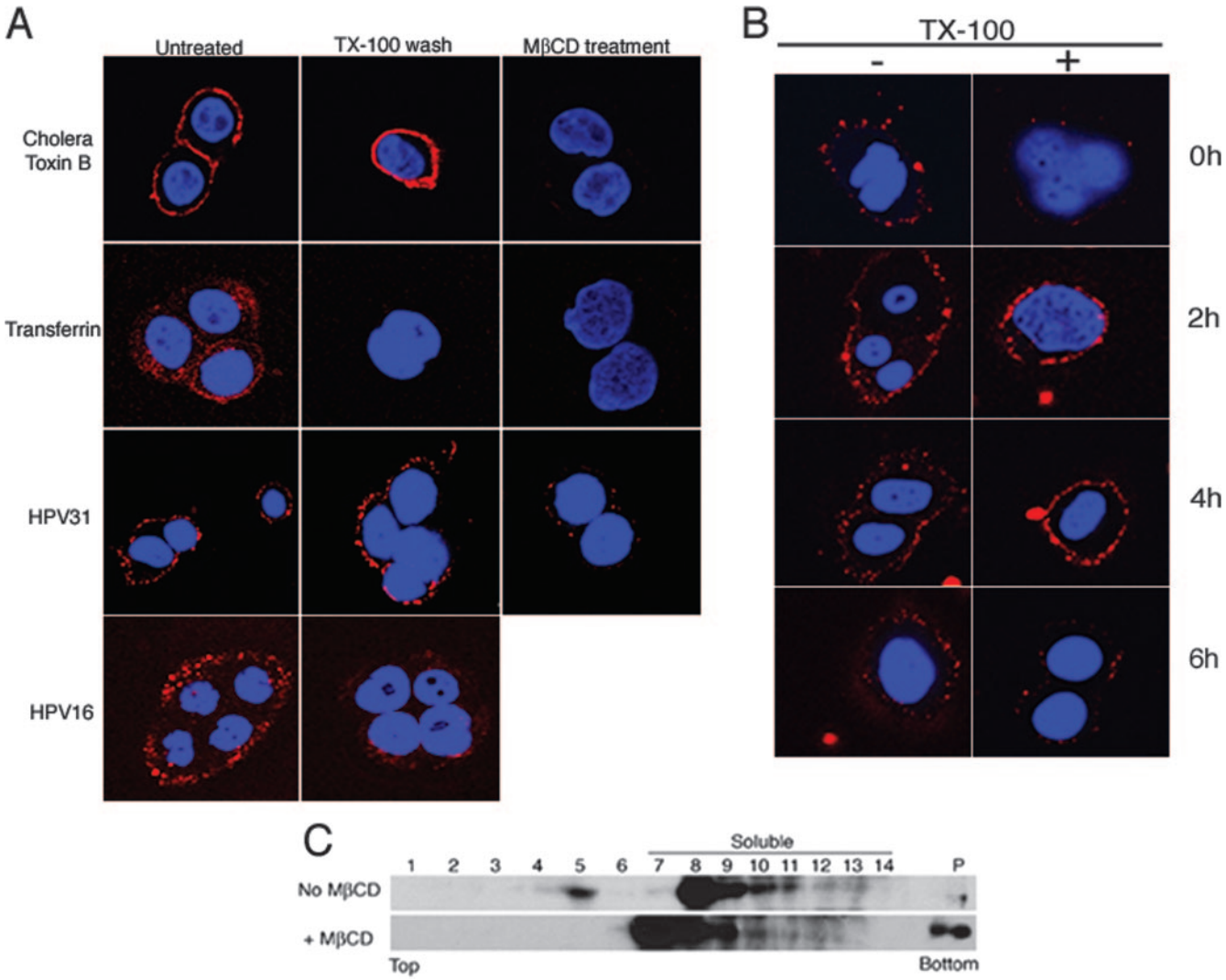

FIG. 5. HPV31 associates with detergent-resistant lipid rafts. (A) AF594-labeled ligands (CT-B, TF, HPV31, or HPV16) were bound to HaCaT cells for 1 h at 4°C and then washed and refed with regular growth medium before incubation at 37°C for 30 min. MβCD treatment for 30 min at 37°C was performed to disrupt cholesterol (right column). Cells were subjected to a control PBS wash (left column) or TX-100 wash (middle and right columns) on ice to remove detergent-soluble membranes. Cells were then fixed and stained with DAPI to visualize nuclei. (B) AF594-HPV31 was bound to cells for 1 h at 4°C and then washed, refed with regular growth medium, and placed at 37°C. At indicated times postattachment, cells were subjected to a control PBS wash (left column) or TX-100 wash (right column) before fixation. (C) HPV31 was bound to HaCaT cells for 1 h at 4°C, and cells were washed and refed with normal growth medium before incubation at 37°C for 30 min in the presence or absence of MβCD. Cells were then lysed, and the samples were subjected to centrifugation on a discontinuous density gradient. Fractions were collected from the top and from pelleted protein (P) and analyzed for HPV31 L1 protein by Western blotting.

formed a TX-100 washout experiment (12). CT-B is known to use caveola-mediated entry and associate with DRMs (23), whereas TF is a ligand that is internalized by clathrin-mediated endocytosis independent of DRMs (24). AF594-labeled CT-B and TF proteins were used as controls. Labeled ligands were bound to HaCaT cells for 1 h at 4°C and then placed at 37°C for 30 min in the presence or absence of MβCD, a cholesterol and DRM disruptor (28). Cells were then washed with TX-100 on ice to remove detergent soluble membranes, fixed, and visualized by confocal microscopy. As expected, CT-B displayed resistance to TX-100 treatment (Fig. 5A, top row), and all CT-B signal was lost following cholesterol disruption by MβCD treatment. TF does not associate with DRM, and as expected, TX-100 treatment removed all AF594-TF (Fig. 5A, second row). AF594-HPV31 displayed strong DRM association, as demonstrated by resistance to TX-100 washout (Fig. 5A, third row), and MβCD treatment confirmed cholesterol dependence for viral signal retention. AF594-labeled HPV16 (Fig. 5A, bottom row) was also tested for its resistance to TX-100 washout at 30 min postattachment. Although some signal was retained following the TX-100 wash, the majority was lost, suggesting that HPV16 binding to HKs does not occur at lipid rafts. HPV31-DRM association was also examined over time (Fig. 5B). DRM association was low immediately following attachment (0 h), increased over time (2 to 4 h), and then decreased at later time points (6 h). HPV31 association with

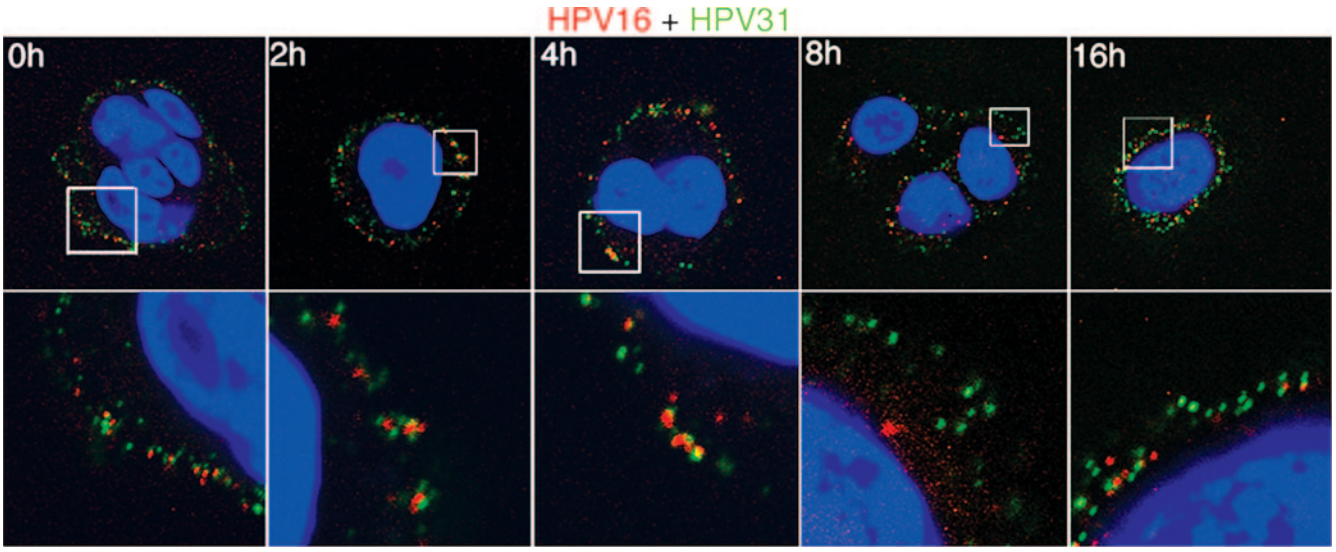

FIG. 6. HPV31 and HPV16 fail to colocalize during HK entry. AF594-HPV16 (red) and AF488-HPV31 (green) virions (each at 10,000 vge/cell) were added to HaCaT cells for 1 h at 4°C, and cells were washed, refed with regular growth medium, and placed at 37°C. At the indicated time points, cells were fixed, DAPI stained, and visualized by confocal microscopy. Lower panels are higher magnifications of boxed areas in each upper panel.

DRM is consistent with a caveola-mediated pathway for HPV31 entry in HKs.

Another lipid raft characteristic due to their specific lipid composition is a density lower than that of soluble plasma membrane components (45). We thus investigated the density of HPV31-membrane interactions as a second means of determining HPV31 association with lipid rafts. Virions were bound to cells for 1 h at 4°C prior to incubation at 37°C for 30 min in the presence or absence of MβCD. Cell lysates were loaded under a discontinuous density gradient and subjected to high-speed centrifugation. Lipid rafts and their associated ligands typically float up in the gradient and are detected in lower-density fractions, separate from soluble fractions. Indeed, a fraction of the HPV31 L1 signal was detected in lower-density fractions (Fig. 5C, top panel, fractions 4 and 5), although a significant amount was still present in soluble fractions. Since a predominant proportion of HPV31 virions remain associated with the extracellular matrix at this time p.i., we interpret the excess virions detected in the soluble fractions to be those that are extracellular matrix associated. Importantly, MβCD treatment completely disrupted the virus signal present in the low-density fractions, confirming the cholesterol requirement for HPV31 association with low-density lipid rafts (Fig. 5C, bottom panel). Together, the data in Fig. 5 confirm the association of HPV31 with lipid rafts at the plasma membrane of HKs prior to entry.

HPV31 and HPV16 do not colocalize during entry into HKs. The findings that HPV31 entry is slow and uses a caveola-dependent pathway involving dynamin 2 and lipid rafts differ significantly from the clathrin-dependent entry pathway reported for HPV16 (5, 13) and from our observations of HPV16 in HKs. Furthermore, the data imply HPV31 and HPV16 virions may use distinct cellular entry pathways in HKs. The nature of HPV virion binding to the HK extracellular matrix (8) and the vastly different internalization times for HPV16 and HPV31 on the plasma membrane have prevented us from performing informative VLP-virion competition experiments for evaluating whether one virus type can block authentic infection of the other as measured by virus gene expression in the HKs. However, we labeled HPV31 virions with AF488 (green) and HPV16 virions with AF594 (red) and monitored plasma membrane binding and entry into HKs over time (Fig. 6). No significant colocalization of the two viral types was observed at any time during the binding and entry process. In fact, at later time points (8 h) and as expected from the observed differences in $t_{1/2}$ for each virus, HPV16 (red) was observed at a perinuclear location within cells, while the HPV31 signal (green) remained at the cell surface. Observation of AF594-labeled HPV31 and AF488-labeled HPV31 entry displayed high levels of colocalization, confirming that particles entering by the same pathway would be expected to display colocalization by microscopy (data not shown). These data suggest that the bulk of observable HPV31 and HPV16 virions enter HKs via distinct pathways.

DISCUSSION

HPVs have coexisted with humans over millions of years via persistent infections and have therefore evolved means of immune evasion involving low gene expression and tightly regulated life cycles in their target tissues, the differentiating epithelium of HKs. These aspects have made it challenging to study early infection events because it is difficult to obtain high-titer virion stocks and to detect experimental infections in HKs. To avoid these obstacles, many researchers have used VLPs and PsVs with nonrelevant cell types for examining initial HPV-cell interactions. Such studies have generated conflicting data regarding attachment requirements (i.e., HSPG interactions), receptor usage (i.e., α6-integrin), endocytic entry (whether clathrin or caveola mediated), and internalization

kinetics. The range of cell types used may partially explain the disparate results. Here we have used authentic HPV31 virions to investigate the entry pathway into HKs, including human foreskin keratinocytes and human cervical keratinocytes, which are the naturally infected host cell type in vivo. Additionally, we utilized both visual and infectious entry assays to confirm our findings.

The new methodology for HPV virion production (41) allowed us to obtain high titers of authentic HPV31. We found that HPV31 entry in HKs is very slow, requiring more than 16 h for completion. This long internalization time for HPV31 is similar to that observed for HPV11, HPV40, and cottontail rabbit papillomavirus (6, 10), although it differs from that for HPV16 (Fig. 2C) (13). This remarkably long internalization time suggests that multiple events may occur upon viral attachment before internalization. Transfer of virions from an initial attachment receptor to an internalization receptor, conformational changes in the viral particle and/or the viral receptor, lipid raft clustering, and signaling events have been widely reported for the internalization of many viruses (reviewed in references 31 and 46) and are possible events that may occur prior to HPV entry as well. Additionally, transfer of papillomavirus from an extracellular matrix component to a plasma membrane receptor may be required, an event that could also affect internalization kinetics (9, 14).

Here we show that HPV31 uses a caveola-mediated pathway that is dynamin 2 dependent for HK entry. We demonstrate that HPV31 and HPV16 have differential sensitivities to chlorpromazine and filipin treatments, suggesting that they are using distinct entry pathways. Our results are consistent with the observations of Bousarghin et al. using PsVs to transduce COS-7 cells (5), but differ from those recently reported by Hindmarsh and Laimins using PsVs in COS-7 and 293TT cells (27). In agreement with a caveola-dependent entry pathway for HKs, we also find that HPV31 associates with lipid rafts as early as 30 min following attachment, suggesting a role for cell surface signaling in entry. Indeed signaling upon VLP binding has been reported for HPVs (17, 19, 38).

Our data indicate that HPV31 may use a cellular entry pathway distinct from that used by HPV16 in their normal host cell, the human epithelial keratinocyte. Consistent with this possibility, we find the two viruses displayed markedly different internalization rates, are differentially susceptible to endocytic inhibitor treatment, differ in their association with DRMs, and fail to colocalize in HKs over 16 h postattachment and internalization. Therefore, the two viral types appear to use independent entry pathways upon infection of HKs. A difference in internalization pathway, were it shown to influence the ability to establish infection, might help explain the difference in prevalences of infections with these two viruses in the population. This work emphasizes the importance of using cells relevant to in vivo infections and demonstrates the diverse nature of the interaction of HPVs with their hosts.

Endocytic routes were previously thought of as strictly defined and distinct in that non-clathrin/noncaveola-mediated endocytosis and clathrin-mediated entry deliver particles to the early endosome, where they then reach late endosomes. Caveola-mediated routes typically pass through the caveosome (bypassing endosomes) and then move to the Golgi body and/or endoplasmic reticulum (44). However, exceptions occur, and each trafficking ligand may have distinct routes in a given cell (25). For example, JC virus enters cells by clathrin-dependent endocytosis, is transported immediately to early endosomes, and is then sorted to a caveolin 1-positive endosomal compartment; this is the first example of clathrin-early endosome-to-caveosome sorting (42). Alternatively, some caveolar vesicles join the early endosomes rather than caveosomes (25). Therefore, it will be important to determine which organelles are involved in the trafficking and uncoating of these two virus types, and we are pursuing experiments to this end. Furthermore, the entry receptor for these two oncogenic viruses has not been unequivocally confirmed and it will be important to determine whether HPV16 and HPV31 utilize different molecules to penetrate host cells. Such results might have implications for design and assessment of antivirals and expanded-spectrum vaccines to target multiple HPV types.

ACKNOWLEDGMENTS

We thank N. Fusenig (DKFZ, Heidelberg, Germany) for HaCaT cells; R. Fichorova (Harvard, Cambridge, MA) for Ect1 and End1 cells; C. Wheeler (University of New Mexico, Albuquerque) for human foreskin keratinocytes; A. Helenius (ETH, Zürich, Switzerland), A. Benmerah (Hôpital Necker-Enfants Malades, Paris, France), and M. McNiven (Mayo Clinic, Rochester, MN) for plasmids encoding wild-type and dominant-negative proteins tagged with GFP; T. Kanda (National Institute of Infectious Diseases, Tokyo, Japan) for the HPV31 L1/L2-expressing plasmid; M. Müller (DKFZ, Heidelberg, Germany) for HPV16 L1 and L2 expression plasmids; N. Christensen (Pennsylvania State University College of Medicine, Hershey) for HPV VLP monoclonal antibodies; R. Roden (Johns Hopkins, Baltimore, MD) for polyclonal HPV31 L1 antisera; and C. Buck and J. Schiller (NIH, Bethesda, MD) for plasmids and advice on PsV production.

This work was supported by NIH grant CA085747 (M.A.O.), NRSA postdoctoral fellowship F32 CA123842 (S.K.C.), and NIH training grant T32 AI07538 (S.K.C. and J.L.S.).

Images in this paper were generated in the University of New Mexico Cancer Center Fluorescence Microscopy Facility, supported as detailed on the web page http://hsc.unm.edu/crtc/microscopy/facility.html. We thank Rebecca Lee and Genevieve Phillips for assistance with confocal microscopy and Steve Jett for assistance with electron microscopy.

All three authors designed the study and analyzed results. J.L.S. and S.K.C. performed research; J.L.S. and M.A.O. wrote the paper.

There are no conflicts of interest for the authors of this study.

REFERENCES

1. **Anderson, H., Y. Chen, and L. Norkin.** 1996. Bound simian virus 40 translocates to caveolin-enriched membrane domains, and its entry is inhibited by drugs that selectively disrupt caveolae. Mol. Biol. Cell **7:**1825–1834.
2. **Benmerah, A., M. Bayrou, N. Cerf-Bensussan, and A. Dautry-Varsat.** 1999. Inhibition of clathrin-coated pit assembly by an Eps15 mutant. J. Cell Sci. **112:**1303–1311.
3. **Bosch, F., M. Manos, N. Munoz, M. Sherman, A. Jansen, J. Peto, M. Schiffman, V. Moreno, R. Kurman, K. Shah, et al.** 1995. Prevalence of human papillomavirus in cervical cancer: a worldwide perspective. J. Natl. Cancer Inst. **87:**796–802.
4. **Boukamp, P., R. T. Petrussevska, D. Breitkreutz, J. Hornung, A. Markham, and N. E. Fusenig.** 1988. Normal keratinization in a spontaneously immortalized aneuploid human keratinocyte cell line. J. Cell Biol. **106:**761–771.
5. **Bousarghin, L., A. Touzé, P.-Y. Sizaret, and P. Coursaget.** 2003. Human papillomavirus types 16, 31, and 58 use different endocytosis pathways to enter cells. J. Virol. **77:**3846–3850.
6. **Christensen, N. D., N. M. Cladel, and C. A. Reed.** 1995. Postattachment neutralization of papillomaviruses by monoclonal and polyclonal antibodies. Virology **207:**136–142.
7. **Christensen, N. D., J. Dillner, C. Eklund, J. J. Carter, G. C. Wipf, C. A. Reed, N. M. Cladel, and D. A. Galloway.** 1996. Surface conformational and linear epitopes on HPV-16 and HPV-18 L1 virus-like particles as defined by monoclonal antibodies. Virology **223:**174–184.
8. **Culp, T. D., L. R. Budgeon, and N. D. Christensen.** 2006. Human papillomaviruses bind a basal extracellular matrix component secreted by kerati-

nocytes which is distinct from a membrane-associated receptor. Virology **347:**147–159.
9. **Culp, T. D., L. R. Budgeon, M. P. Marinkovich, G. Meneguzzi, and N. D. Christensen.** 2006. Keratinocyte-secreted laminin 5 can function as a transient receptor for human papillomaviruses by binding virions and transferring them to adjacent cells. J. Virol. **80:**8940–8950.
10. **Culp, T. D., and N. D. Christensen.** 2004. Kinetics of in vitro adsorption and entry of papillomavirus virions. Virology **319:**152–161.
11. **Culp, T. D., N. M. Cladel, K. K. Balogh, L. R. Budgeon, A. F. Mejia, and N. D. Christensen.** 2006. Papillomavirus particles assembled in 293TT cells are infectious in vivo. J. Virol. **80:**11381–11384.
12. **Damm, E.-M., L. Pelkmans, J. Kartenbeck, A. Mezzacasa, T. Kurzchalia, and A. Helenius.** 2005. Clathrin- and caveolin-1-independent endocytosis: entry of simian virus 40 into cells devoid of caveolae. J. Cell Biol. **168:**477–488.
13. **Day, P. M., D. R. Lowy, and J. T. Schiller.** 2003. Papillomaviruses infect cells via a clathrin-dependent pathway. Virology **307:**1–11.
14. **Day, P. M., C. D. Thompson, C. B. Buck, Y.-Y. S. Pang, D. R. Lowy, and J. T. Schiller.** 2007. Neutralization of human papillomavirus with monoclonal antibodies reveals different mechanisms of inhibition. J. Virol. **81:**8784–8792.
15. **D'Souza, G., A. R. Kreimer, R. Viscidi, M. Pawlita, C. Fakhry, W. M. Koch, W. H. Westra, and M. L. Gillison.** 2007. Case-control study of human papillomavirus and oropharyngeal cancer N. Engl. J. Med. **356:**1944–1956.
16. **Eash, S., W. Querbes, and W. J. Atwood.** 2004. Infection of Vero cells by BK virus is dependent on caveolae. J. Virol. **78:**11583–11590.
17. **Evander, M., I. Frazer, E. Payne, Y. M. Qi, K. Hengst, and N. A. J. McMillan.** 1997. Identification of the α_6 integrin as a candidate receptor for papillomaviruses. J. Virol. **71:**2449–2456.
18. **Fichorova, R. N., J. G. Rheinwald, and D. J. Anderson.** 1997. Generation of papillomavirus-immortalized cell lines from normal human ectocervical, endocervical, and vaginal epithelium that maintain expression of tissue-specific differentiation proteins. Biol. Reprod. **57:**847–855.
19. **Fothergill, T., and N. A. J. McMillan.** 2006. Papillomavirus virus-like particles activate the PI3-kinase pathway via alpha-6 beta-4 integrin upon binding. Virology **352:**319–328.
20. **Galloway, C. J., G. E. Dean, M. Marsh, G. Rudnick, and I. Mellman.** 1983. Acidification of macrophage and fibroblast endocytic vesicles in vitro. Proc. Natl. Acad. Sci. USA **80:**3334–3338.
21. **Gillison, M., W. Koch, R. Capone, M. Spafford, W. Westra, L. Wu, M. Zahurak, R. Daniel, M. Viglione, D. Symer, et al.** 2000. Evidence for a casual association between human papillomavirus and a subset of head and neck cancers. J. Natl. Cancer Inst. **92:**709–720.
22. **Giroglou, T., L. Florin, F. Schäfer, R. E. Streeck, and M. Sapp.** 2001. Human papillomavirus infection requires cell surface heparan sulfate. J. Virol. **75:**1565–1570.
23. **Hagmann, J., and P. H. Fishman.** 1982. Detergent extraction of cholera toxin and gangliosides from cultured cells and isolated membranes. Biochim. Biophys. Acta **720:**181–187.
24. **Harder, T., P. Scheiffele, P. Verkade, and K. Simons.** 1998. Lipid domain structure of the plasma membrane revealed by patching of membrane components. J. Cell Biol. **141:**929–942.
25. **Helenius, A.** 2007. Virus entry and uncoating, p. 99–118. *In* D. M. Knipe and P. M. Howley (ed.), Fields virology, 5th ed., vol. 1. Lippincott Williams & Wilkins, Philadephia, PA.
26. **Henley, J. R., E. W. A. Krueger, B. J. Oswald, and M. A. McNiven.** 1998. Dynamin-mediated internalization of caveolae. J. Cell Biol. **141:**85–99.
27. **Hindmarsh, P., and L. Laimins.** 2007. Mechanisms regulating expression of the HPV 31 L1 and L2 capsid proteins and pseudovirion entry. Virol. J. **4:**19.
28. **Ilangumaran, S., and D. Hoessli.** 1998. Effects of cholesterol depletion by cyclodextrin on the sphingolipid microdomains of the plasma membrane. Biochem. J. **335:**433–440.
29. **Kreider, J., M. K. Howett, A. Leure-Dupree, R. J. Zaino, and J. A. Weber.** 1987. Laboratory production in vivo of infectious human papillomavirus type 11. J. Virol. **61:**590–593.
30. **Kurzchalia, T. V., and R. G. Partan.** 1999. Membrane microdomains and caveolae. Curr. Opin. Cell Biol. **11:**424–431.
31. **Marsh, M., and A. Helenius.** 2006. Virus entry: open sesame. Cell **124:**729–740.
32. **Meyers, C., M. Frattini, J. Hudson, and L. Laimins.** 1992. Biosynthesis of human papillomavirus from a continuous cell line upon epithelial differentiation. Science **257:**971–973.
33. **Ochoa, G.-C., V. I. Slepnev, L. Neff, N. Ringstad, K. Takei, L. Daniell, W. Kim, H. Cao, M. McNiven, R. Baron, and P. De Camilli.** 2000. A functional link between dynamin and the actin cytoskeleton at podosomes. J. Cell Biol. **150:**377–390.
34. **Oh, P., D. P. McIntosh, and J. E. Schnitzer.** 1998. Dynamin at the neck of caveolae mediates their budding to form transport vesicles by GTP-driven fission from the plasma membrane of endothelium. J. Cell Biol. **141:**101–114.
35. **Ozbun, M. A.** 2002. Human papillomavirus type 31b infection of human keratinocytes and the onset of early transcription. J. Virol. **76:**11291–11300.
36. **Ozbun, M. A.** 2002. Infectious human papillomavirus type 31b: purification and infection of an immortalized human keratinocyte cell line. J. Gen. Virol. **83:**2753–2763.
37. **Patterson, N. A., J. L. Smith, and M. A. Ozbun.** 2005. Human papillomavirus type 31b infection of human keratinocytes does not require heparan sulfate. J. Virol. **79:**6838–6847.
38. **Payne, E., M. R. Bowles, A. Don, J. F. Hancock, and N. A. J. McMillan.** 2001. Human papillomavirus type 6b virus-like particles are able to activate the Ras-MAP kinase pathway and induce cell proliferation. J. Virol. **75:**4150–4157.
39. **Pelkmans, L., J. Kartenbeck, and A. Helenius.** 2001. Caveolar endocytosis of simian virus 40 reveals and new two-step vesicular-transport pathway to the ER. Nat. Cell Biol. **3:**473–483.
40. **Pho, M. T., A. Ashok, and W. J. Atwood.** 2000. JC virus enters human glial cells by clathrin-dependent receptor-mediated endocytosis. J. Virol. **74:**2288–2292.
41. **Pyeon, D., P. F. Lambert, and P. Ahlquist.** 2005. Production of infectious human papillomavirus independently of viral replication and epithelial cell differentiation. Proc. Natl. Acad. Sci. USA **102:**9311–9316.
42. **Querbes, W., B. A. O'Hara, G. Williams, and W. J. Atwood.** 2006. Invasion of host cells by JC virus identifies a novel role for caveolae in endosomal sorting of noncaveolar ligands. J. Virol. **80:**9402–9413.
43. **Reading, S. A., and N. J. Dimmock.** 2007. Neutralization of animal virus infectivity by antibody. Arch. Virol. **152:**1047–1059.
44. **Sieczkarski, S. B., and G. R. Whittaker.** 2004. Viral entry. Curr. Top. Microbiol. Immunol. **285:**1–23.
45. **Simons, K., and E. Ikonen.** 1997. Functional rafts in cell membranes. Nature **387:**569–572.
46. **Smith, A. E., and A. Helenius.** 2004. How viruses enter animal cells. Science **304:**237–242.
47. **Takei, K., P. S. McPherson, S. L. Schmid, and P. D. Camilli.** 1995. Tubular membrane invaginations coated by dynamin rings are induced by GTP-γS in nerve terminals. Nature **374:**186–190.
48. **Wang, L. H., K. G. Rothberg, and R. G. Anderson.** 1993. Mis-assembly of clathrin lattices on endosomes reveals a regulatory switch for coated pit formation. J. Cell Biol. **123:**1107–1117.